





# Eugenol Nanoparticles Ameliorate Doxorubicin-Induced Spermatogenic Dysfunction by Inhibiting the PINK1/Parkin and BNIP3/NIX Signaling Pathways

Yang Fu <sup>1,2</sup>, Peipei Yuan <sup>1,2</sup>, Manyv Wang<sup>1</sup>, Yajuan Zheng<sup>1</sup>, Yan Zhang<sup>1</sup>, Lirui Zhao<sup>1</sup>, Qingyun Ma<sup>1</sup>, Pengsheng Wang<sup>1</sup>, Xiaotian Sun<sup>1</sup>, Xiaoke Zheng <sup>1,2</sup>, Weisheng Feng <sup>1,2</sup>

<sup>1</sup>Department of Pharmacy, Henan University of Chinese Medicine, Zhengzhou 450046, China, Zhengzhou, 450046, People's Republic of China; <sup>2</sup>The Engineering and Technology Center for Chinese Medicine Development of Henan Province, Zhengzhou, 450046, People's Republic of China

Correspondence: Xiaoke Zheng; Weisheng Feng, Department of Pharmacy, Henan University of Chinese Medicine, The Engineering and Technology Center for Chinese Medicine Development of Henan Province, 156 Jinshui East Road, Zhengzhou, 450046, People's Republic of China, Email zhengxk.2006@163.com; fwsh@hactcm.edu.cn

**Purpose:** Doxorubicin (DOX) precipitates cell apoptosis in testicular tissues, and it is imperative to develop drugs to alleviate the spermatogenic disorders it causes. *Eugenia caryophyllata* Thunb is often used to treat male sexual disorders. Eugenol, a major component of *Eugenia caryophyllata* Thunb. has inadequate stability and low solubility, which limits its pharmacological effects. Eugenol nanoparticles (NPs) (ENPs) are expected to overcome these limitations. The protective effects of ENPs against DOX-induced reproductive toxicity were studied in mice.

**Methods:** Eugenol was encapsulated in Methoxy-Poly(ethylene glycol)-Poly(lactide-co-glycolide) nanoparticles (mPEG-PLGA-NPs), and their role in ameliorating spermatogenic dysfunction was verified in vivo and in vitro.

**Results:** We present a promising delivery system that encapsulates eugenol into mPEG-PLGA-NPs and forms them into nanocomposites. In vitro, ENPs significantly reduced doxorubicin-induced ROS and inflammatory factors in GC-1 cells and regulated the expression of the mitochondrial autophagy protein PINK1 and meiosis-related protein SCP3. In vivo, ENPs significantly increased sperm motility in mice, reduced apoptosis and oxidative stress in the testes, inhibited the testicular PINK1/Parkin and BNIP3/NIX signaling pathways, and enhanced the expression of factors associated with meiosis.

**Conclusion:** Given their safety and efficacy, these ENPs have potential application prospects in mitigating doxorubicin-induced spermatogenic dysfunction.

**Keywords:** Eugenol nanoparticles, Doxorubicin, spermatogenic dysfunction, PINK1/Parkin and BNIP3/NIX signaling pathways, Mitochondrial autophagy

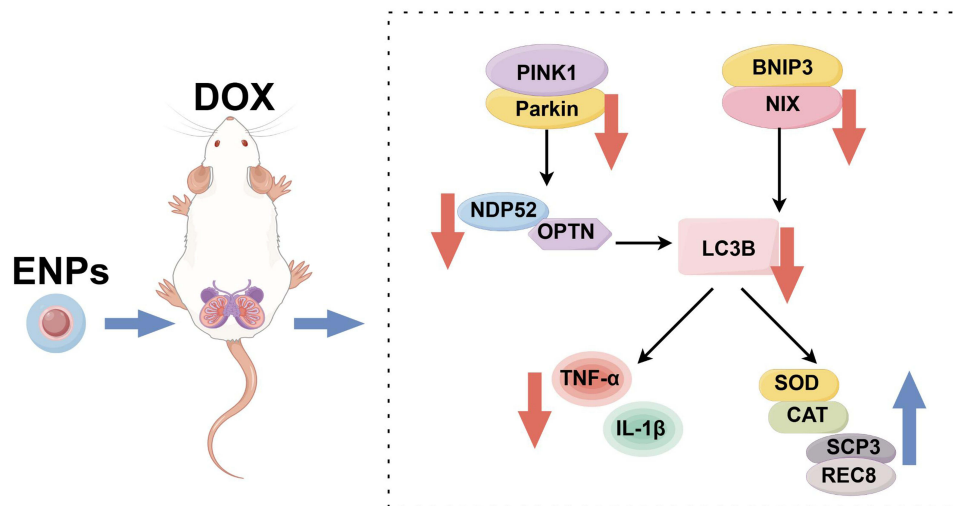
## Introduction

Doxorubicin specifically targets rapidly dividing cells, where it triggers chromosomal abnormalities in spermatogonia, arrests the cell cycle, and promotes apoptosis. This process leads to impaired spermatogenesis and ultimately results in male infertility.<sup>1,2</sup> Due to its effectiveness for cancer treatment, doxorubicin continues to be the top choice for managing and mitigating cancer-related complications.<sup>3</sup>

Facing the demand of patients for doxorubicin and the significant side effects of doxorubicin in cancer treatment, preventing and alleviating spermatogenic disorders caused by the toxic side effects of doxorubicin chemotherapy, and seeking preventive and therapeutic drugs are related to the health and quality of life of the people.

*Eugenia caryophyllata* Thunb has been used as a native remedy for treating male sexual disorders in Asian countries.<sup>4</sup> Eugenol is the main component of *Eugenia caryophyllata* Thunb.<sup>5</sup> It can inhibit oxidative stress levels in the testes in rats

## Graphical Abstract



with diabetes<sup>6</sup> and improve testicular toxicity caused by nitrate and acrylamide.<sup>7,8</sup> Eugenol improved the hormone production and antioxidant defense in rat testing after exposure to the chemotherapy drug cisplatin. However, its protective effect on spermatogenic disorders caused by doxorubicin remains to be studied. Given that its poor water solubility and low bioavailability limit its application, we examined the protective effects of eugenol nanoparticles (ENPs) on Doxorubicin -induced spermatogenic dysfunction in vitro and in vivo.

## Material and Methods

### Chemicals

Eugenol was obtained from Shanghai Yuanye Biotechnology Co. Ltd. (Shanghai, China). Methoxy-Poly(ethylene glycol)-Poly(lactide-co-glycolide) (mPEG-PLGA; molecular weight (MW) = 18 kDa; LA/GA = 50:50; PEG MW = 2 kDa) was purchased from Jinan Daigang Biomaterials (Jinan, China). Poly (vinyl alcohol) (PVA; MW = 30–70 kDa; HD, 80%) and doxorubicin were obtained from Shanxi PUDE Pharmaceutical Co. Ltd. (Shanxi, China). All other chemicals and reagents utilized were of analytical grade.

### Preparation of ENPs

Briefly, the eugenol aqueous solution (50 mg/mL) was combined with the PLGA dichloromethane (DCM) solution (40 mg/mL) in a 1:12 volume ratio. Following 1 minute of ultrasonication in an ice bath, the mixture was dispersed within a 1% PVA aqueous solution, maintaining a 1:8 volume ratio. It was further treated with ultrasonication for 5 minutes using an ice bath. The emulsion was stirred for 2 h to obtain a stable double emulsion. DCM was evaporated to obtain a suspension of ENPs. Large particles were removed by centrifugation at 2500× g for 2 min at 4°C and at 6000× g for 10 min at 4°C to obtain ENPs. The unsealed drugs and impurities were removed by washing twice with water. The precipitate was dispersed in physiological saline and stored at 4°C.

### Characterization Studies of ENPs

The Nano ZS ZEN 3600 employs dynamic light scattering (Malvern, UK) to assess the polydispersity index (PDI), mean particle size, and size distribution of ENPs. The test sample was diluted tenfold for measurement. Each sample was measured in triplicate.

The morphology of particle size was observed using transmission electron microscopy. The SEM images of the ENPs were viewed using a Scanning Electron Microscope (JEOL, Japan, 200kv).<sup>9</sup> A small-animal in vivo imaging system (Pearl™ Imager, LI-COR, USA) was used to detect the distribution of OIL-NPs in vivo.<sup>10</sup>

## Evaluation of the Encapsulation Efficiency of ENPs

We dissolved 30 mg of ENPs in 3 mL of 90% methanol and further sonicated it for 5 min to break down the nanoparticles and release encapsulated eugenol. The resulting solution was centrifuged at  $10,000 \times g$ , and the supernatant was collected. The absorbance of the supernatant was measured to quantify eugenol at 280 nm using a spectrophotometer (Thermo, MA, USA).<sup>11</sup>

## Cell Culture

A spermatogonia cell line from mice (GC-1) was obtained from the American Type Culture Collection (Manassas, VA, USA). Cells were cultured in high glucose Dulbecco's modified Eagle medium supplemented with 10% fetal bovine serum, 1% l-glutamine, and 1% penicillin-streptomycin mixture. Cells were incubated at 37°C in a humidified atmosphere with 5% carbon dioxide.

## Determination of ROS and Cell Viability

GC-1 cells were seeded uniformly into 96-well plates at a concentration of  $2 \times 10^4$ /mL or into 6-well plates at a concentration of  $4 \times 10^4$ /mL. The normal group was cultured under standard conditions, whereas the model group and other groups underwent damage with 0.25  $\mu$ M doxorubicin for 24 hours. The ENPs-L and ENPs-H groups were treated with ENPs (5 or 10 nM of eugenol). The levels of ROS in the cells were determined by staining with the DCFH-DA probe and employing an appropriate assay kit from Elabscience (Wuhan, China). Cell viability was assessed using the Cell Counting Kit (CCK)-8 assay (Abcam, Cambridge, UK), and absorbance was measured at 450 nm.

## Evaluation of the Mitochondrial Autophagy Protein and Meiosis-Related Protein in GC-1 Cells Using a High-Content Imaging System

The GC-1 cells were seeded in 96-well plates (E190236X; PerkinElmer) at a density of  $2 \times 10^4$  cells/mL. The levels of PTEN-induced putative kinase 1 (PINK1, 1:100 dilution; 6946; Cell Signaling Technology, Danvers, MA, USA) and synaptonemal complex protein (SCP) 3 were detected (1:100 dilution; 23024-1-AP; Proteintech, Wuhan, China). The cells were scanned using a high-throughput imaging system (Opera Phenix, PerkinElmer, USA) and the relative protein expression levels were normalized using Harmony 4.8 high-throughput imaging and analysis software (PerkinElmer: Waltham, Massachusetts, USA).<sup>12,13</sup>

## Animal Model

Forty Kunming mice ( $25 \pm 2$  g) were purchased from Beijing Victoria Experimental Animal Center (Beijing, China). Approval for the use of animals for experimental purposes was obtained from SCXK (Beijing, 2021-0006). Animal experiments were approved by the Henan University of Traditional Chinese Medicine (Zhengzhou, China) (Ethics No. DWLL201908112). The experiments were performed according to the guidelines and regulations of the Animal Care and Use Committee of the National Organization Engineering Center (Zhengzhou, China).

The mice were randomly divided into four groups ( $n=10$ ): control (CON), doxorubicin-induced injury (model), ENPs-L, and ENPs-H. Mice in the CON and model groups were administered normal saline (10 g/0.1 mL, i.v). Mice in the ENPs-L and ENPs-H groups received intravenous injections of ENPs every three days for 15 days, preceding doxorubicin-induced injury. For each injection, the mice received ENPS-L (0.25mg/kg eugenol-loaded PLGA nanoparticles) or ENPS-H (1.25mg/kg eugenol-loaded PLGA nanoparticles). Doxorubicin (30 mg/kg, i.p.) was administered two days after the final administration.<sup>14,15</sup> All the mice were euthanized two days later. The tissues were stored at  $-80^\circ\text{C}$ .

## Histopathological Evaluation

Following dissection, the testes were fixed in 4% paraformaldehyde overnight, embedded in paraffin, sectioned to a thickness of 5  $\mu\text{m}$ , and mounted on individual glass slides.<sup>16</sup> After hematoxylin and eosin staining, testicular sections were examined under a light microscope (NIKON Eclipse ci, Tokyo, Japan).

## Determination of Sperm Content and Motility

The epididymis was removed and immersed in a physiological saline solution. Following mincing, the sample was incubated at 37°C and filtered through a 70- $\mu\text{m}$  filter using physiological saline. A sperm quality analyzer (Huazhong Medical Products Co., Ltd., Shijiazhuang, China) was used to assess sperm motility. This was followed by fixation of 100  $\mu\text{L}$  of the filtrate in 5 mL of 5%  $\text{NaHCO}_3$ , and the sperms were counted.

## Assessment of Oxidative Stress

Testis tissue samples were homogenized in ice-cold phosphate-buffered saline. The homogenate was centrifuged at 4°C, 15000  $\times g$  for 10 min. The activities of superoxide dismutase (SOD; A006-2-1), malondialdehyde (MDA; A003-1-2), and catalase (CAT; A007-2-1) (Nanjing Jiancheng Bioengineering Institute, China) were determined according to the manufacturer's instructions.

## Immunofluorescence

The levels of the testicular tissue-related proteins PINK1 and Bcl-2/E1B-19kDa interacting protein 3 (BNIP3; 44060; Cell Signaling Technology) were detected. Fluorescent Cy3-coupled secondary antibodies were used for detection.<sup>17</sup>

## Western Blotting

The expression of PINK1, Parkin (1:1000 dilution; 4211; Cell Signaling Technology), Optineurin (OPTN; 1:1000; 58981, Cell Signaling Technology), BNIP3, BCL2/Adenovirus E1B 19 kDa protein-interacting protein 3-like (NIX, 1:1000; 12396; Cell Signaling Technology), SCP3, REC8 meiotic recombination protein (REC8; 1:1000; ab192241; Proteintech), NDP52, nuclear dot protein 52 kDa (NDP52, 1:1000; 60732; Cell Signaling Technology), microtubule-associated protein light chain 3B (LC3B, 1:1000; 3868, Cell Signaling Technology), and Sequestosome 1 (P62, 1:1000; 8025, Cell Signaling Technology) was assayed by Western blotting.<sup>17,18</sup>

## Real-Time RT-qPCR

The RNA were extracted from the testicular tissue or GC-1 cells using the RNA extraction kit (R1200, Solarbio, China). The RNA purity and concentration were determined by measuring absorbance at 260 and 280 nm. Next, the HiScript<sup>®</sup> II first-strand cDNA synthesis kit (D7185; Beyotime, China) was employed to reverse-transcribe 2  $\mu\text{g}$  of total RNA into cDNA. Subsequently, the ChamQ<sup>™</sup> Universal SYBR<sup>®</sup> qPCR Master Mix (Q711-02, Vazyme Biotech, China) was used for PCR. The primer sequences used are listed in Table 1.

## Statistical Analyses

The data are summarized as mean  $\pm$  SD. The data were analyzed using SPSS (version 25.0; IBM, Armonk, NY, USA). Significant differences between groups were determined using one-way ANOVA.  $P < 0.05$  denoted statistical significance.

## Results

### Characterization of ENPs

The maximum loading capacity and efficiency of the ENPs were 5.03 $\pm$ 0.21% and 62.43 $\pm$ 1.76%, respectively. The morphology and distribution of ENPs were determined using transmission electron microscopy and photodynamics. The ENPs were small compact spheres (Figure 1A). The particle size distribution of the ENPs was between 37 and 295 nm, which was consistent with the normal distribution characteristics (Figure 1B).

**Table 1** Primer Sequences

Target	Forward primer (5'–3')	Reverse primer (5'–3')	Accession number	Product size
PINK1	TTCTCCGCCAGTCGGTAG	CTGCTTCTCCTCGATCAGCC	NM_026880.2	141
PARKIN	GAGGTTCGATTCTGACACCAGC	CCGGCAAAAATCACACGCAG	NM_016694.5	95
NIX	CTGGAGCACGTTCTTCTC	ACAGTGCGAACTGCCTCTTG	NM_009761.4	111
OPT	ATGTCCCATCAACCTCTGAGC	TCAAATCGCCCTTTCATAGCTTG	NM_001356487.1	209
DAZI	ATACCTCCGGCTTATACAACCTGT	GACTTCTTTTGCGGGCCATT	NM_010021.5	128
CYCLIN-I	CAGTTTCCCAATGCTGGTTG	CCTCTGCATACTCCGTTACGTTA	NM_001305221.1	99
SCP3	AGCCAGTAACCAGAAAATTGAGC	CCACTGCTGCAACACATTCATA	NM_011517.2	106
REC8	GGTCATCACCTTACAGGAGGC	TCTGCGATCAGCAGTTCTAAGT	NM_001360390.1	105
TNF- $\alpha$	CTGAACTTCGGGGTGATCGG	GGCTTGCTCACTCGAATTTGAGA	NM_013693.3	122
IL-1 $\beta$	GAAATGCCACCTTTTGACAGTG	TGGATGCTCTCATCAGGACAG	NM_008361.4	116
GAPDH	TGTGTCCGTCGTGGATCTGA	TTGCTGTTGAAGTCGCAGGAG	NM_008084.3	150

The Polydispersity Index of the ENP suspension was  $<0.2$ . This suggests the successful construction of the ENP nanoparticles. In vivo imaging of small animals showed that ENPs were accumulated in the testes of mice 24 h after drug administration (Figure 1C).

## Effect of ENPs on the ROS and Survival and Inflammatory Factors of GC-1 Cells Damaged by Doxorubicin

Doxorubicin markedly increased the ROS levels in GC-1 cells and markedly decreased their survival rate ( $P < 0.01$ ), whereas ENPs effectively decreased ROS levels and enhanced cell survival ( $P < 0.01$ ) (Figure 2A–C).

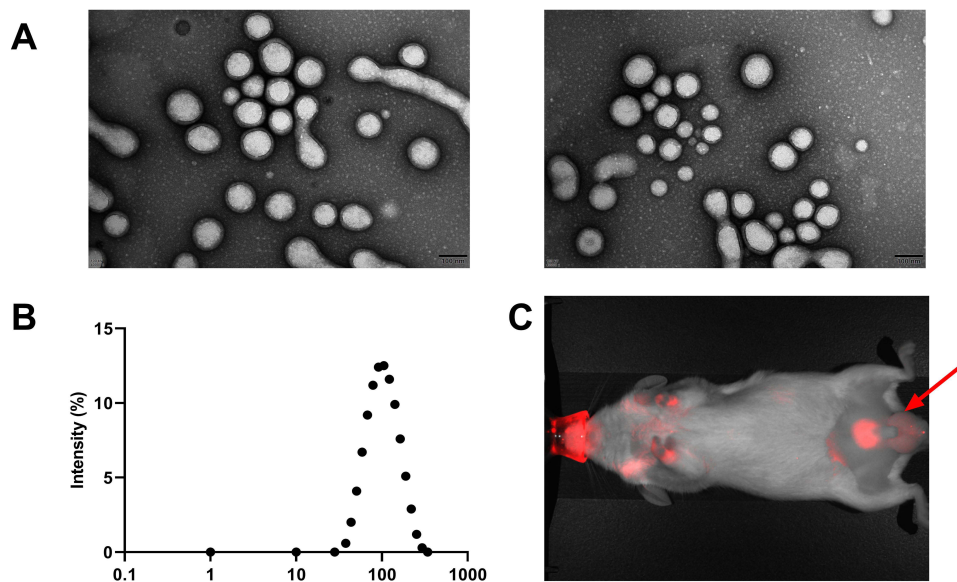


**Figure 1** Characterization of ENPs: (A) ENPs transmission electron microscope. (B) Dynamic light scattering of Eugenol nanoparticles (ENPs) and (C) in vivo distribution and targeting of ENPs. Black arrows mark showing that accumulation of ENP in the testes.

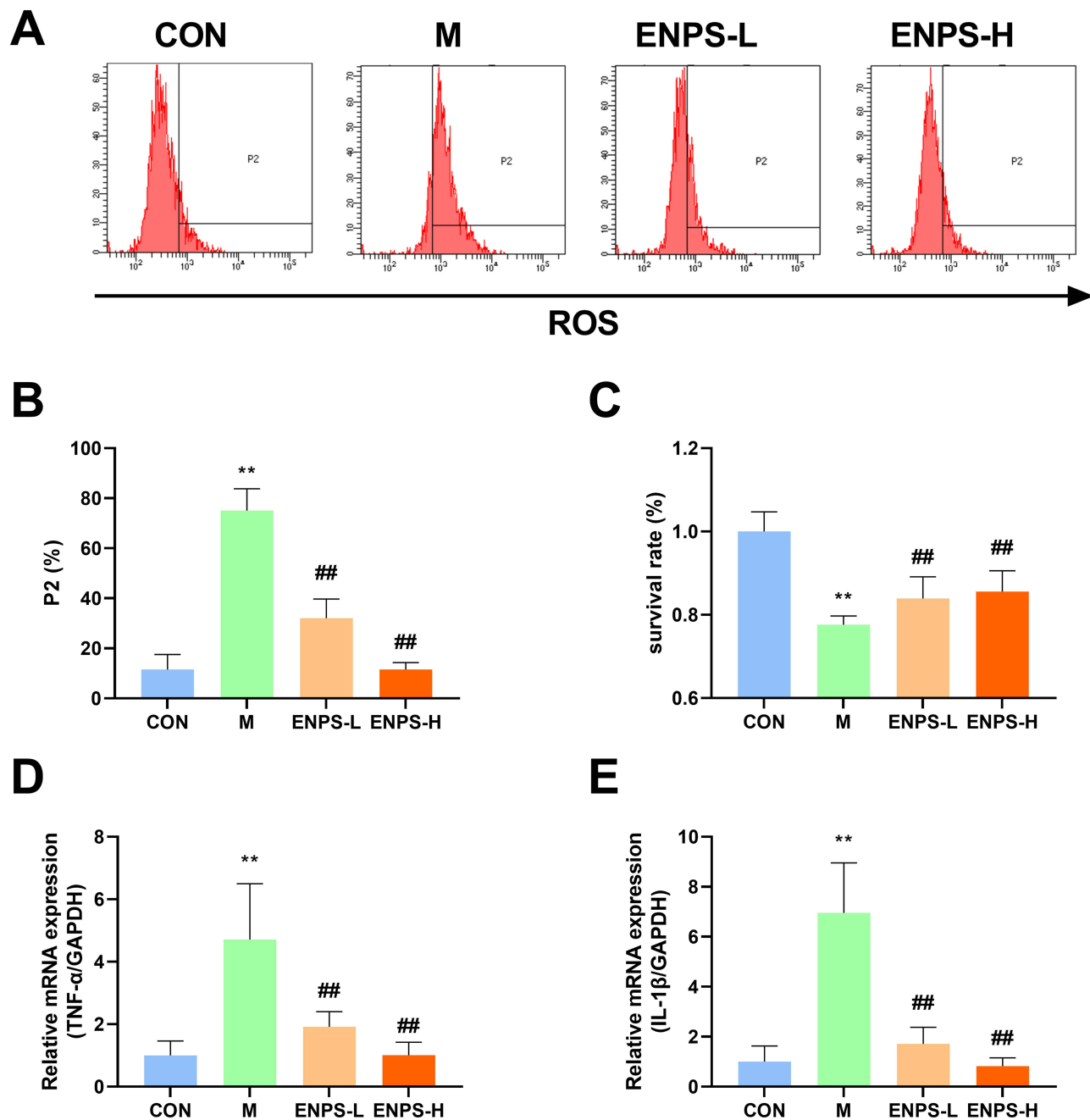


**Figure 2** Effect of ENPs on the ROS, survival and inflammatory factors of GC-1 cells: (A–C) Effect of ENPs on percent apoptosis and survival of GC-1 cells in each group. (D) (E) Effects of ENPs on mRNA expression of TNF- $\alpha$  and IL-1 $\beta$  in GC-1 cells.

**Notes:** Data are the mean  $\pm$  SD ( $n = 6$ ). \*\* $P < 0.01$  vs the CON group. ## $P < 0.01$  vs the Model group.

**Abbreviations:** CON, control group underwent standard culture; M, model group; ENPS-L, 0.5 $\mu$ M Eugenol-loaded PLGA nanoparticles; ENPS-H, 1 $\mu$ M Eugenol-loaded PLGA nanoparticles; TNF- $\alpha$ , tumor necrosis factor- $\alpha$ ; IL-1 $\beta$ , interleukin-1 $\beta$ .

Furthermore, ENPs markedly suppressed the mRNA expression of TNF- $\alpha$  and IL-1 $\beta$  in GC-1 cells ( $P < 0.01$ ) (Figure 2D and E). These findings confirm that ENPs can significantly mitigate ROS levels and enhance the survival of GC-1 cells damaged by doxorubicin, while reducing the levels of inflammatory cytokines.

## Effect of ENPs on the Mitochondrial Autophagy Protein PINK1 and Meiosis-Related Protein SCP3 of GC-1 Cells Damaged by Doxorubicin

The effects of ENPs on the mitochondrial autophagy protein PINK1 and the meiosis-related protein SCP3 in GC-1 cells damaged by doxorubicin were detected using a high-connotation imaging system. Compared with the normal group, the PINK1 protein level in the model group was significantly increased while the SCP3 protein level was significantly decreased ( $P < 0.01$ ). ENPs significantly reversed the levels of PINK1 and SCP3 ( $P < 0.01$ ) (Figure 3).

## Effects of ENPs on Bodyweight, Testicular Indices, Testes Histology, and Sperm Motility of Doxorubicin-Treated Mice

Testicular structure and the number of spermatogenic cells in the CON group were normal. Doxorubicin reduced the thickness of germ cell layer and cell shedding in mouse testicular tissues. Compared with the model group, the ENPs-L and ENPs-H groups demonstrated a significant increase in germ cell layers and showed improved cell shedding (Figure 4). No abnormal deaths occurred in any group. There were no significant differences in bodyweights among

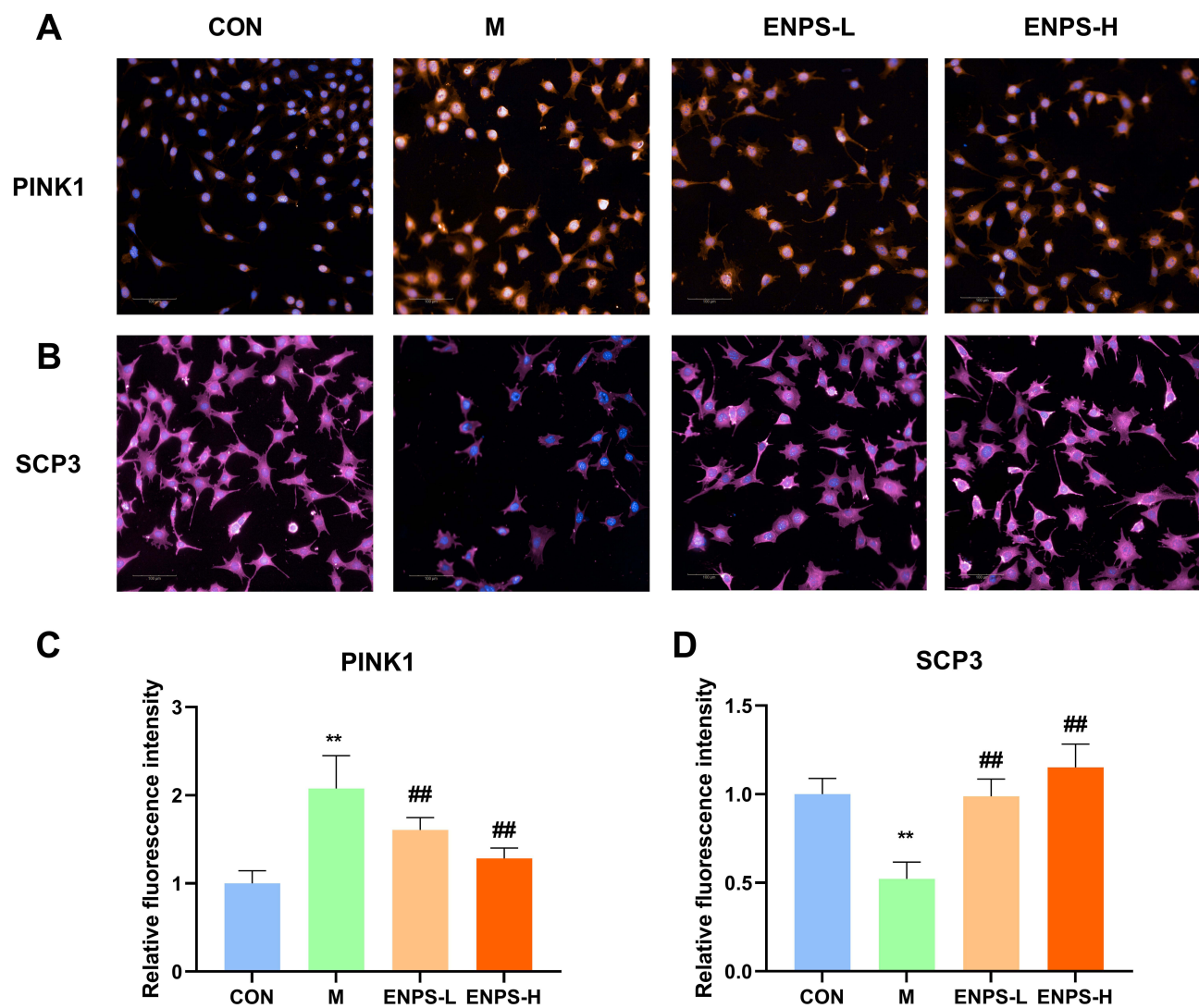


**Figure 3** Effect of ENPs on the Mitochondrial autophagy protein PINK1 and meiosis-related protein SCP3 in GC-1 cells damaged by doxorubicin: (A–D) Protein expression of PINK1 and SCP3 in GC-1 cells, scale bar 50  $\mu$ m.

**Notes:** Data are the mean  $\pm$  SD (n = 6). \*\* $P < 0.01$  vs the CON group. ### $P < 0.01$  vs the Model group.

**Abbreviations:** CON, control group underwent standard culture; M, model group; ENPS-L, 0.5 $\mu$ M Eugenol-loaded PLGA nanoparticles; ENPS-H, 1 $\mu$ M Eugenol-loaded PLGA nanoparticles; PINK1, PTEN-induced putative kinase 1; SCP3, small C-terminal domain phosphatase 3.

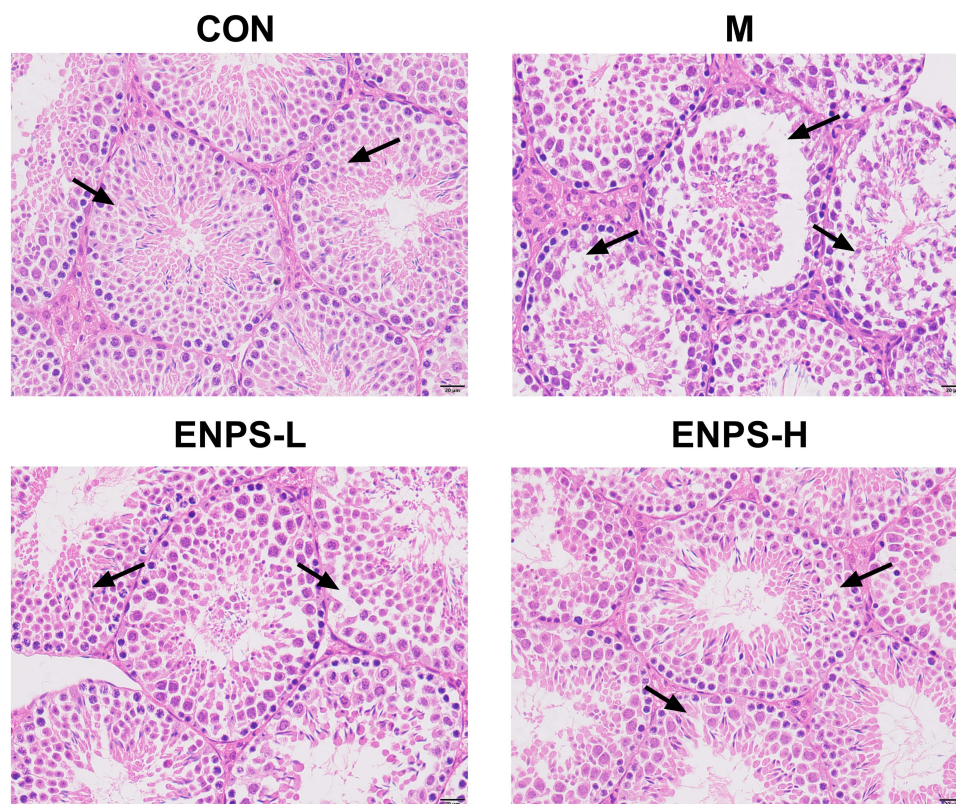


**Figure 4** Effect of ENPs on testicular histology in mice. The CON group showed a normal organizational structure. The Model group showed cell shedding and a decrease in the spermatogenic-cell layer. Compared with the Model group, the ENPS-L group and ENPS-H group had significantly improved histology, and the ENPS-H group had the best effect. Black arrows mark showing spermatogenic cell layers.

**Abbreviations:** CON, Control group; M, Model group with 30 mg/kg Adriamycin, i.p.; ENPS-L, 0.25 mg/kg PSE, i.v.; ENPS-H, 1.25 mg/kg PSE-PLGAs, i.v.

the four groups (Figure 5A). Figure 5B and C display the effect of ENPs on testicular and epididymal indices (representing the ratio of testicular or epididymal weight to bodyweight) in mice. The testicular and epididymal indices in the model group significantly decreased ( $P < 0.01$ ), whereas those in the ENPS-H group significantly increased ( $P < 0.01$ ). Doxorubicin significantly reduced the number of sperms and sperm motility in mice ( $P < 0.01$ ), whereas ENPs significantly increased sperm count and motility ( $P < 0.01$ ); ENPS-H had a better effect (Figure 5D and E).

### Effect of ENPs on Oxidative Stress

Treatment with doxorubicin led to a significant reduction in the levels of SOD and CAT, while concurrently increasing the levels of MDA ( $P < 0.01$ ) (Figure 5F–H). ENPs restored SOD and CAT levels and reduced MDA levels ( $P < 0.01$ ). Our findings suggest that ENPs reduce oxidative stress in DOX-treated mice.

### Effect of ENPs on Percent Apoptosis, Mitochondrial Membrane Potential, and Inflammatory Factors in the Testicular Cells of Doxorubicin-Treated Mice

Apoptosis and mitochondrial membrane potential in testicular cells were detected using flow cytometry. Doxorubicin significantly increased the percentage of apoptotic cells and mitochondrial membrane potential of testicular cells ( $P < 0.01$ ). The ENPs significantly reduced the percentage of apoptotic cells by regulating mitochondrial membrane potential ( $P < 0.05$ ,  $P < 0.01$ ) (Figure 6A–D). RT-qPCR revealed that doxorubicin upregulated the mRNA expressions of TNF- $\alpha$  and IL-1 $\beta$  ( $P < 0.01$ ), whereas ENPs significantly inhibited them ( $P < 0.05$ ,  $P < 0.01$ , respectively) (Figure 6E and F).



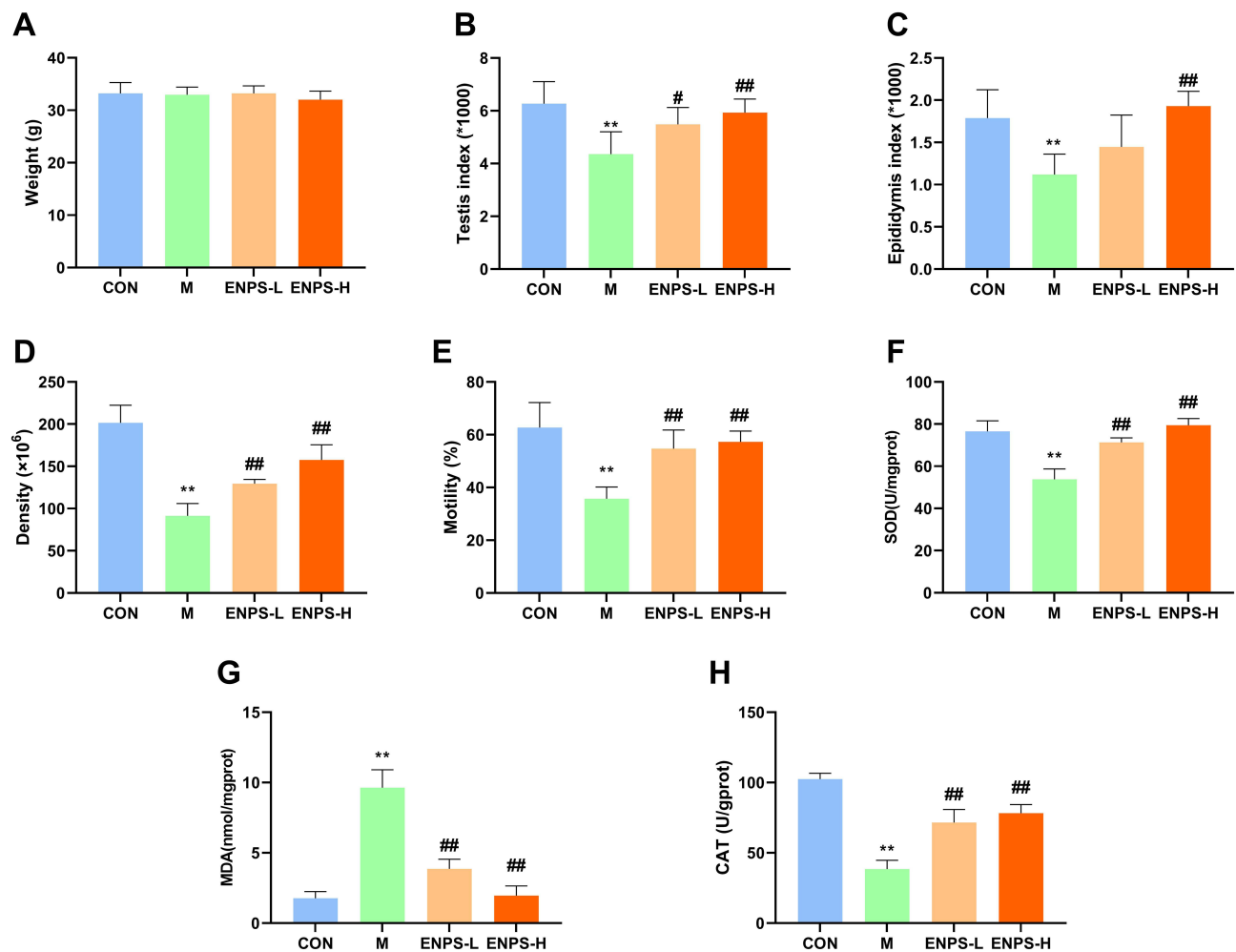


**Figure 5** Effects of ENPs on bodyweight, testicular indices, and sperm motility of doxorubicin-treated mice. Effect of ENPs on (A) bodyweight, (B) testicular indices, (C) Epididymis indices, (D) sperm count, (E) motility, (F) SOD, (G) MDA and (H) CAT of doxorubicin-treated mice.

**Notes:** Data are the mean  $\pm$  SD (n = 6). \*\* $P < 0.01$  vs the CON group. # $P < 0.05$  and ## $P < 0.01$  vs the Model group.

**Abbreviations:** CON, Control group; M, Model group with 30 mg/kg Adriamycin, i.p.; ENPS-L, 0.25 mg/kg PSE, i.v.; ENPS-H, 1.25 mg/kg PSE-PLGAs, i.v.

## Effects of ENPs on the PINK1/Parkin and BNIP3/NIX Signaling Pathways and Meiosis-Related Indices in the Testes of Doxorubicin-Treated Mice

Using Western blotting, we assessed the expressions of proteins associated with the PINK1/Parkin and BNIP3/NIX signaling pathways in the testes of mice across all groups. Relative to the control group, the expressions of PINK1, Parkin, OPTN, BNIP3, NIX, NDP52, and LC3B markedly increased in the model group, whereas the expression of P62 markedly decreased ( $P < 0.05$ ,  $P < 0.01$ ). Treatment with ENPs significantly decreased the expressions of these proteins and increased the expression of P62 ( $P < 0.05$  or  $P < 0.01$ , respectively) (Figure 7A). We used Real-time RT-qPCR to measure the mRNA expressions of PINK1/Parkin and BNIP3/NIX signaling pathway-related proteins. The mRNA expressions of PINK1, Parkin, OPTN and NIX in the model group was significantly higher than that in the control group ( $P < 0.01$ ). The ENPs reversed these effects ( $P < 0.05$  or  $P < 0.01$ , respectively) (Figure 7B). Furthermore, we detected the PINK1 and BNIP3 levels using immunofluorescence, which was consistent with the results of WB and RT-qPCR (Figure 7C).

Doxorubicin significantly suppressed the expressions of SCP3 and REC8 ( $P < 0.01$ ) (Figure 7A), whereas treatment with the ENPs markedly enhanced the expressions of SCP3 and REC8 ( $P < 0.01$ ). We also assessed the mRNA levels of other meiotic proteins deleted in azoospermia, protein (Daz) 1, and CYCLIN-D1. Compared with the control group, the

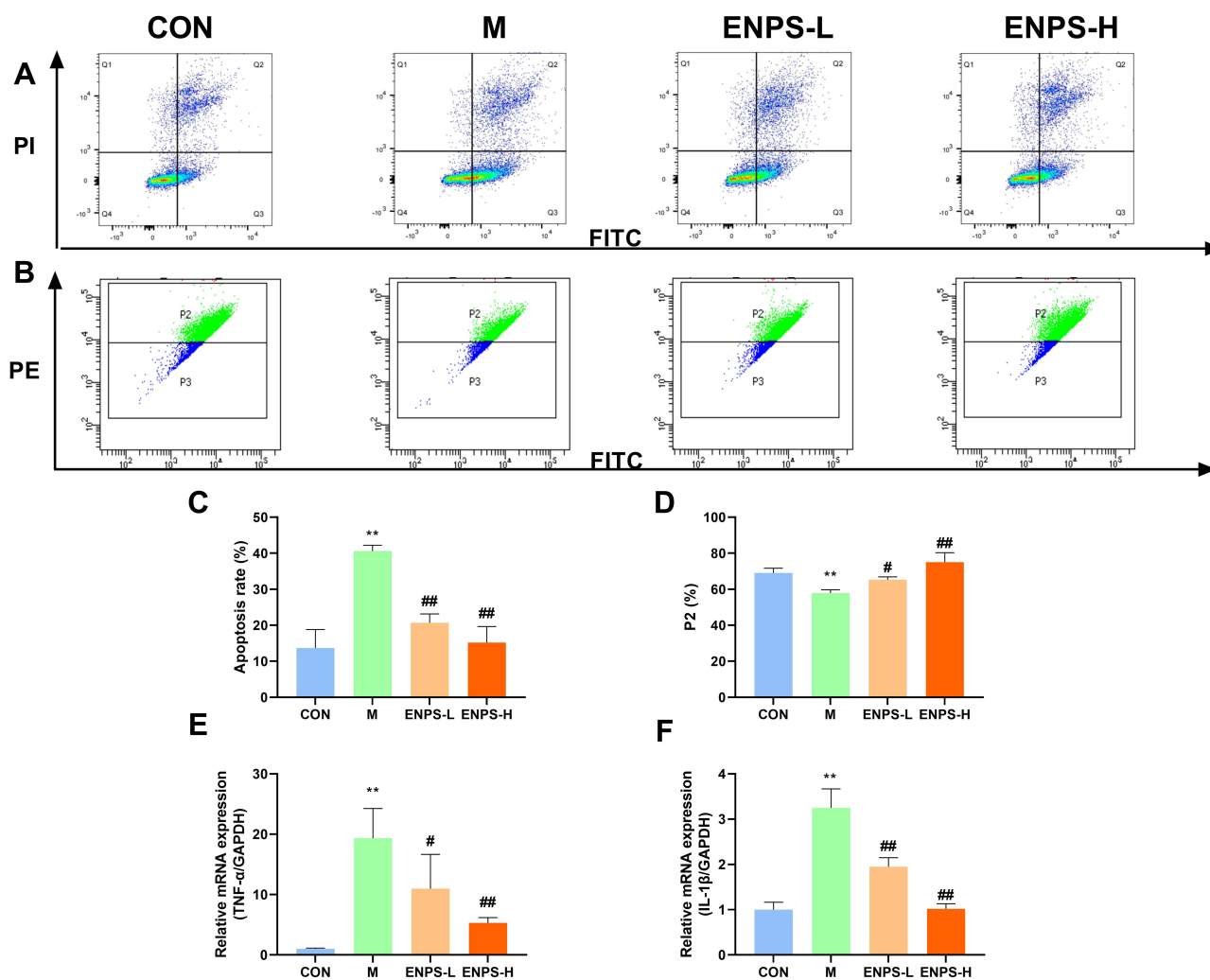


**Figure 6** Effects of ENPs percent apoptosis, mitochondrial membrane potential and inflammatory factors in mouse testicular cells: **(A–C)** Percent apoptosis in the testicular tissue of mice in each group. **(B–D)** Effects of ENPs on mitochondrial membrane potential in the testicular tissue of mice in each group. **(E and F)** mRNA expression of TNF- $\alpha$  and IL-1 $\beta$  in the testicular tissue of mice each group measured by RT-qPCR.

**Notes:** Data are the mean  $\pm$  SD (n = 6). \*\* $P < 0.01$  vs the CON group. # $P < 0.05$  and ## $P < 0.01$  vs the Model group.

**Abbreviations:** CON, Control group; M, Model group with 30 mg/kg Adriamycin, i.p.; ENPS-L, 0.25 mg/kg PSE, i.v.; ENPS-H, 1.25 mg/kg PSE-PLGAs, i.v.; TNF- $\alpha$ , tumor necrosis factor- $\alpha$ ; IL-1 $\beta$ , interleukin-1 $\beta$ .

expressions of these genes in the model group was significantly reduced ( $P < 0.01$ ) (Figure 7B), but ENP treatment markedly increased them ( $P < 0.01$ ).

## Discussion

Adriamycin, a first-line chemotherapeutic drug, is used to treat various cancers. However, it has severe side effects and can cause testicular damage.<sup>19</sup> *Eugenia caryophyllata* Thunb is used to treat male infertility.<sup>4</sup> Studies have shown that eugenol can improve sperm motility.<sup>6</sup> It is metabolized readily and has a short half-life in vivo,<sup>20</sup> and eugenol was used to develop ENPs. PLGA has good biocompatibility, safety, and stability. Reproductive toxicity has not been reported and compared with that of other metallic materials. MPEG-PLGA block copolymers are amphiphilic.<sup>21</sup> The nanoparticles are coated with a hydrophilic PEG layer, enabling them to circumvent macrophage clearance and bolster the therapeutic effectiveness of the loaded drugs. Consequently, PEG-PLGA was selected for drug loading. The final nanoparticles diameters of approximately 105 nm, with good PDI, encapsulation efficiency, and drug loading. ENPs were accumulated in the testes of mice, which helps eugenol exert its therapeutic effect.

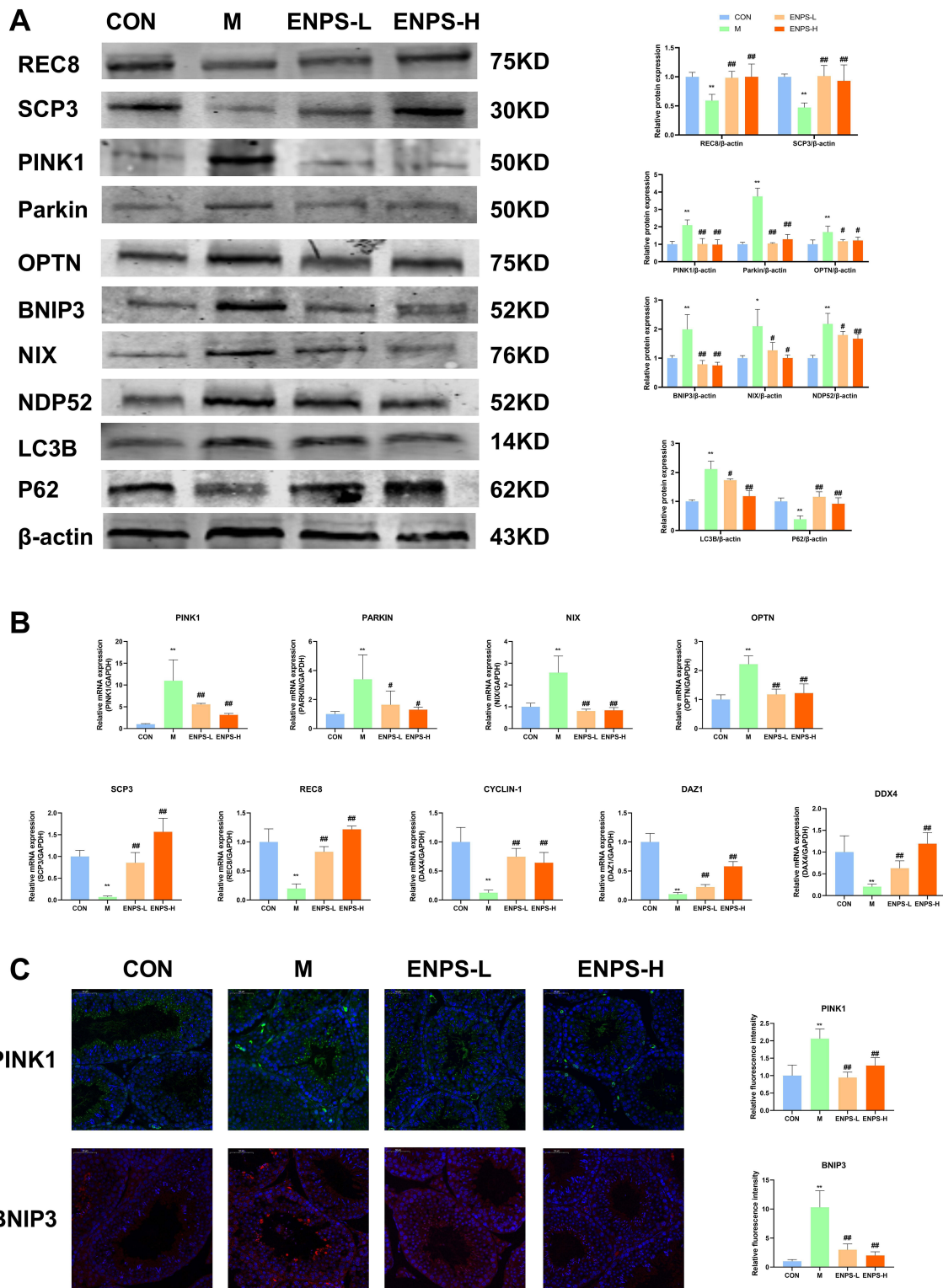


**Figure 7** Effects of ENPs on the PINK1/Parkin signaling pathway and meiosis-related indices in the testes of doxorubicin-treated mice. **(A)** Protein and **(B)** mRNA expression of PINK1/Parkin and BNIP3/NIX signaling pathway and meiosis-associated proteins in the testicular tissue of mice in each group was measured by Western blotting and RT-qPCR. **(C)** The protein expression of PINK1 and SCP3 in the testicular tissue of mice in each group was measured by Immunofluorescence, scale bar 50  $\mu$ m.

**Notes:** Data are the mean  $\pm$  SD (n = 6). \* $P$  < 0.05 and \*\* $P$  < 0.01 vs the CON group. # $P$  < 0.05 and ### $P$  < 0.01 vs the Model group.

**Abbreviations:** CON, Control group; M, Model group with 30 mg/kg Adriamycin, i.p.; ENPS-L, 0.25 mg/kg PSE, i.v.; ENPS-H, 1.25 mg/kg PSE-PLGAs, i.v.; PINK1, PTEN-induced putative kinase 1; OPT, Optineurin; BNIP3, Bcl-2/E1B-19kDa interacting protein 3; NIX, BCL2/Adenovirus E1B 19 kDa protein-interacting protein 3-like; NDP52, nuclear dot protein 52 kDa; LC3B, microtubule-associated protein light chain 3B; P62, Sequestosome 1; SCP3, small C-terminal domain phosphatase 3; REC8: meiotic recombination protein; DAZ1: deleted in azoospermia protein 1.

Doxorubicin led to increased ROS levels in GC-1 cells, but ENPs significantly reduced the ROS levels and significantly inhibited the levels of the inflammatory factors TNF- $\alpha$  and IL-1  $\beta$ . This improved the survival rate of GC-1 cells. In this study, we used a high-content imaging system to detect the expressions of the PNIK1 signaling pathway and meiosis-related proteins. We found that ENPs significantly inhibited the expression of PNIK1 and increased the expression of SCP3. These results confirmed that ENPs could effectively inhibit cell apoptosis, regulate the PNIK1 signaling pathway, and promote the level of meiotic division proteins. Therefore, we conducted *in vivo* experiments to further explore the mechanism of action of the ENPs.

Post-administration, we found that the ENPs did not significantly affect the bodyweight of the mice. Doxorubicin significantly reduced testicular and epididymal coefficients in mice, inhibited sperm motility, and decreased sperm counts. ENPs significantly increased testicular and epididymal coefficients, total sperm count, and sperm motility. Mitochondria play a crucial role in testicular tissue; they are associated with the proliferation, division, and apoptosis of germ cells. The decline in mitochondrial membrane potential corresponds to the early stages of cell apoptosis.<sup>22</sup> We used flow cytometry to observe the levels of testicular cell apoptosis and mitochondrial membrane potential. The results indicated that ENPs significantly inhibited testicular cell apoptosis and enhanced the mitochondrial membrane potential.

Oxidative stress is regarded as the initial event in reproductive toxicity. Consequently, MDA accumulates excessively as a marker of lipid peroxidation, while SOD and CAT become depleted as the primary ROS scavengers.<sup>23,24</sup> TNF- $\alpha$  mediates doxorubicin apoptosis by activating IL-1 $\beta$ .<sup>25</sup> ADM can cause significant apoptosis and oxidative stress in GC-1 cells; promote the expressions of TNF- $\alpha$ , IL-1 $\beta$ , and MDA; and downregulate the expressions of SOD and CAT. ENPs significantly increased the expressions of antioxidant-related proteins and reduced the excessive increase in apoptosis-related protein expression.

Mitochondria are highly sensitive to oxidative damage mediated by ROS. Mitochondria are not only one of the main sites for DOX metabolism, but are also the preferred target for DOX-mediated attacks.<sup>26</sup> Mitochondria also destabilize the functioning of cells, tissues, and organs. The classic mitophagy pathways consist of the ubiquitin-dependent pathway mediated by PINK1-Parkin and the ubiquitin-independent pathway mediated by non-Parkin-dependent mitochondrial receptor proteins.<sup>27</sup> Research has shown that testicular injury is accompanied by excessive mitophagy in testicular cells.<sup>28,29</sup> Parkin and p62 can recognize and bind to LC3 to form isolation membranes and trigger lysosomes to degrade damaged mitochondria.<sup>30</sup> BNIP3 interferes with mitochondrial dynamics by promoting the division of damaged mitochondria.<sup>31</sup> In addition, BNIP3/NIX interacts with LC3 to accelerate autophagy and degradation.<sup>32</sup> LC3 is a specific marker of mitophagy.<sup>33</sup> P62 is a classic receptor for autophagy involved in proteasomal degradation of ubiquitinated proteins.<sup>34</sup> In response to stress, the adaptor protein P62 identifies phosphorylated ubiquitin chains as the initial signal for binding to LC3B and mitosis. OPTN is a prototypical selective autophagy receptor capable of escorting ubiquitinated substrates to autophagosomes for degradation.<sup>35</sup> In addition to P62, NDP52 is a newly identified key protein related to autophagy that binds to microtubule-associated LC3 on the autophagic surface.<sup>36</sup> We found that doxorubicin overactivates mitochondrial autophagy in the testes, accompanied by the upregulation of the PINK1/Parkin and BNIP3/NIX pathways. ENPs significantly inhibited the PINK1/Parkin and BNIP3/NIX signaling pathways and mitigated the excessive activation of mitochondrial autophagy.

Excessive ROS activates mitochondrial autophagy, thereby impeding spermatogenesis.<sup>37–39</sup> We found that DOX significantly inhibited the expression of SCP3 in mice testes, and ENPs improved the expression of SCP3. We also assessed the levels of proteins associated with meiosis in sperm, specifically REC8, DAZ1, DDX4, and CYCLIN-D1.<sup>40–42</sup> We discovered that ENPs significantly improved the expressions of meiosis-related genes.

## Conclusion

Our results suggest that ENPs ameliorate doxorubicin-induced spermatogenic dysfunction. This action may be associated with the inhibition of the PINK1/Parkin and BNIP3/NIX signaling pathways and may augment the expression of factors related to meiosis. The clinical application of ENPs deserves further research.

## Acknowledgments

The graphical abstract was created using FigDraw.

## Funding

This work was supported by the National Key Research and Development Program (Major Project for Research of the Modernization of TCM; 2019YFC1708802) and Henan Province High-Level Personnel Special Support (“Zhongyuan One Thousand People Plan”; Zhongyuan Leading Talent (ZYQR201810080)).

## Disclosure

The authors report no conflicts of interest in this work.

## References

1. Ibrahim RYM, Mansour SM, Elkady WM. Phytochemical profile and protective effect of *Ocimum basilicum* aqueous extract in doxorubicin/irradiation-induced testicular injury. *J Pharm Pharmacol*. 2020;72(1):101–110. doi:10.1111/jphp.13175
2. Babalola AA, Adelowo AR, Da-Silva OF, et al. Attenuation of doxorubicin-induced hypothalamic-pituitary-testicular axis dysfunction by diphenyl diselenide involves suppression of hormonal deficits, oxido-inflammatory stress and caspase 3 activity in rats. *J Trace Elem Med Biol*. 2023;79:127254. doi:10.1016/j.jtemb.2023.127254
3. Lengyel CG, Habeeb BS, Altuna SC, Trapani D, Khan SZ, Hussain S. The Global Landscape on the Access to Cancer Medicines for Breast Cancer: the ONCOLLEGE Experience. *Cancer Treat Res*. 2023;188:353–368. doi:10.1007/978-3-031-33602-7\_14
4. Mishra RK, Singh SK. Safety assessment of *Syzygium aromaticum* flower bud (clove) extract with respect to testicular function in mice. *Food Chem Toxicol*. 2008;46(10):3333–3338. doi:10.1016/j.fct.2008.08.006
5. Gad AF, Abdelgalil GM, Radwan MA. Bio-molluscicidal potential and biochemical mechanisms of clove oil and its main component eugenol against the land snail, *Theba pisana*. *Pestic Biochem Physiol*. 2023;192:105407. doi:10.1016/j.pestbp.2023.105407
6. Chilukoti SR, Sahu C, Jena G. Protective role of eugenol against diabetes-induced oxidative stress, DNA damage, and apoptosis in rat testes. *J Biochem Mol Toxicol*. 2024;38(1):e23593. doi:10.1002/jbt.23593
7. Saleh DO, Baraka SM, Jaleel GAA, Hassan A, Ahmed-Farid OA. Eugenol alleviates acrylamide-induced rat testicular toxicity by modulating AMPK/p-AKT/mTOR signaling pathway and blood-testis barrier remodeling. *Sci Rep*. 2024;14(1):1910. doi:10.1038/s41598-024-52259-1
8. Rajini SV, Sarjan HN S. Ameliorative action of eugenol on nitrate induced reproductive toxicity in male rats. *Toxicol Rep*. 2024;13:101702. doi:10.1016/j.toxrep.2024.101702
9. Xu R, Wang J, Xu J, et al. Rhynchophylline Loaded-mPEG-PLGA Nanoparticles Coated with Tween-80 for Preliminary Study in Alzheimer's Disease. *Int J Nanomed*. 2020;15:1149–1160. doi:10.2147/ijn.s236922
10. Zheng Y, Yuan P, Zhang Z, et al. Fatty Oil of *Descurainia Sophia* Nanoparticles Improve Monocrotaline-Induced Pulmonary Hypertension in Rats Through PLC/IP3R/Ca<sup>2+</sup> Signaling Pathway. 2023;18:7483–7503. doi:10.2147/ijn.s436866
11. Li P, Bukhari SNA, Khan T, et al. Apigenin-Loaded Solid Lipid Nanoparticle Attenuates Diabetic Nephropathy Induced by Streptozotocin Nicotinamide Through Nrf2/HO-1/NF-kB Signalling Pathway. *Int J Nanomed*. 2020;15:9115–9124. doi:10.2147/ijn.s256494
12. Fu Y, Yuan PP, Zheng YJ, et al. Ephedra herb reduces Adriamycin-induced testicular toxicity by upregulating the gonadotropin-releasing hormone signalling pathway. *Biomed Pharmacother*. 2022;150:113061. doi:10.1016/j.biopha.2022.113061
13. Fu Y, Yuan PP, Zheng YJ, et al. Pseudoephedrine Nanoparticles Alleviate Adriamycin-Induced Reproductive Toxicity Through the GnRHR Signaling Pathway. *Int J Nanomed*. 2022;17:1549–1566. doi:10.2147/ijn.s348673
14. Fedato RP, Maistro EL. Absence of genotoxic effects of the coumarin derivative 4-methylscutellin in vivo and its potential chemoprevention against doxorubicin-induced DNA damage. *J Appl Toxicol*. 2014;34(1):33–39. doi:10.1002/jat.2823
15. Fouad AA, Refaie MMM, Abdelghany MI. Naringenin palliates cisplatin and doxorubicin gonadal toxicity in male rats. *Toxicol Mech Methods*. 2019;29(1):67–73. doi:10.1080/15376516.2018.1512180
16. Zhou Y, Ji J, Zhuang J, Wang L, Hong F. Nanoparticulate TiO<sub>2</sub> Induced Suppression of Spermatogenesis is Involved in Regulatory Dysfunction of the cAMP-CREB/CREM Signaling Pathway in Mice. *J Biomed Nanotechnol*. 2019;15(3):571–580. doi:10.1166/jbn.2019.2704
17. Fu Y, Yuan PP, Cao YG, et al. Geniposide in *Gardenia jasminoides* var. *radicans* Makino modulates blood pressure via inhibiting WNK pathway mediated by the estrogen receptors. *J Pharm Pharmacol*. 2020;72(12):1956–1969. doi:10.1111/jphp.13361
18. Gao L, Yuan P, Zhang Q, et al. Taxifolin improves disorders of glucose metabolism and water-salt metabolism in kidney via PI3K/AKT signaling pathway in metabolic syndrome rats. *Life Sci*. 2020;263:118713. doi:10.1016/j.lfs.2020.118713
19. Smart E, Lopes F, Rice S, et al. Chemotherapy drugs cyclophosphamide, cisplatin and doxorubicin induce germ cell loss in an in vitro model of the prepubertal testis. *Sci Rep*. 2018;8(1):1773. doi:10.1038/s41598-018-19761-9
20. Wijewantha N, Sane S, Eikanger M, et al. Enhancing Anti-Tumorigenic Efficacy of Eugenol in Human Colon Cancer Cells Using Enzyme-Responsive Nanoparticles. *Cancers*. 2023;15(4). doi:10.3390/cancers15041145
21. Khalil NM, Do Nascimento TC, Casa DM, et al. Pharmacokinetics of curcumin-loaded PLGA and PLGA-PEG blend nanoparticles after oral administration in rats. *Colloids Surf B Biointerfaces*. 2013;101:353–360. doi:10.1016/j.colsurfb.2012.06.024
22. Chen K, Wu L, Liu Q, et al. Glutathione improves testicular spermatogenesis through inhibiting oxidative stress, mitochondrial damage, and apoptosis induced by copper deposition in mice with Wilson disease. *Biomed Pharmacother*. 2023;158:114107. doi:10.1016/j.biopha.2022.114107
23. Hasgul R, Uysal S, Haltas H, et al. Protective effects of Ankaferd blood stopper on aspirin-induced oxidative mucosal damage in a rat model of gastric injury. *Toxicol Ind Health*. 2014;30(10):888–895. doi:10.1177/0748233712466134
24. Keshta AT, Fathallah AM, Attia YA, Salem EA, Watad SH. Ameliorative effect of selenium nanoparticles on testicular toxicity induced by cisplatin in adult male rats. *Food Chem Toxicol*. 2023;179:113979. doi:10.1016/j.fct.2023.113979
25. Yang CC, Chen YT, Chen CH, Chiang JY, Zhen YY, Yip HK. Assessment of doxorubicin-induced mouse testicular damage by the novel second-harmonic generation microscopy. *Am J Transl Res*. 2017;9(12):5275–5288.
26. Yin J, Guo J, Zhang Q, et al. Doxorubicin-induced mitophagy and mitochondrial damage is associated with dysregulation of the PINK1/parkin pathway. *Toxicol In Vitro*. 2018;51:1–10. doi:10.1016/j.tiv.2018.05.001

27. Bai H, Fang Y, Cao H, et al. Inhibition of the BNIP3/NIX-dependent mitophagy aggravates copper-induced mitochondrial dysfunction in duck renal tubular epithelial cells. *Environ Toxicol: Int J.* 2023;38(3):579–590. doi:10.1002/tox.23704
28. Li Q, Yang Q, Guo P, et al. Mitophagy contributes to zinc-induced ferroptosis in porcine testis cells. *Food Chem Toxicol.* 2023;179:113950. doi:10.1016/j.fct.2023.113950
29. Liang C, Gao Y, He Y, et al. Fluoride induced mitochondrial impairment and PINK1-mediated mitophagy in Leydig cells of mice: in vivo and in vitro studies. *Environ Pollut.* 2020;256:113438. doi:10.1016/j.envpol.2019.113438
30. Wang S, Deng Z, Ma Y, et al. The Role of Autophagy and Mitophagy in Bone Metabolic Disorders. *Int J Biol Sci.* 2020;16(14):2675–2691. doi:10.7150/ijbs.46627
31. Zhang J, Ney PA. Role of BNIP3 and NIX in cell death, autophagy, and mitophagy. *Cell Death Differ.* 2009;16(7):939–946. doi:10.1038/cdd.2009.16
32. Tang C, Han H, Liu Z, et al. Activation of BNIP3-mediated mitophagy protects against renal ischemia-reperfusion injury. *Cell Death Dis.* 2019;10(9):677. doi:10.1038/s41419-019-1899-0
33. Schaaf MB, Keulers TG, Vooijs MA, Rouschop KM. LC3/GABARAP family proteins: autophagy-(un)related functions. *FASEB j.* 2016;30(12):3961–3978. doi:10.1096/fj.201600698R
34. Tao M, Liu T, You Q, Jiang Z. p62 as a therapeutic target for tumor. *Eur J Med Chem.* 2020;193:112231. doi:10.1016/j.ejmech.2020.112231
35. Liu ZZ, Hong CG, Hu WB, et al. Autophagy receptor OPTN (optineurin) regulates mesenchymal stem cell fate and bone-fat balance during aging by clearing FABP3. *Autophagy.* 2021;17(10):2766–2782. doi:10.1080/15548627.2020.1839286
36. Viret C, Rozières A, Faure M. Novel Insights into NDP52 Autophagy Receptor Functioning. *Trends Cell Biol.* 2018;28(4):255–257. doi:10.1016/j.tcb.2018.01.003
37. Liu H, Du X, Zhang Z, et al. Co-exposure of microcystin and nitrite enhanced spermatogenic disorders: the role of mtROS-mediated pyroptosis and apoptosis. *Environ Int.* 2024;188:108771. doi:10.1016/j.envint.2024.108771
38. Li T, Zheng Y, Wu Z, et al. YTHDF2 controls hexavalent chromium-induced mitophagy through modulating Hif1 $\alpha$  and Bnip3 decay via the m(6)A/mRNA pathway in spermatogonial stem cells/progenitors. *Toxicol Lett.* 2023;377:38–50. doi:10.1016/j.toxlet.2023.01.010
39. Yang Q, Liu X, Chen J, et al. Lead-mediated inhibition of lysine acetylation and succinylation causes reproductive injury of the mouse testis during development. *Toxicol Lett.* 2020;318:30–43. doi:10.1016/j.toxlet.2019.10.012
40. Li Q, Qiao D, Song NH, et al. Association of DAZ1/DAZ2 deletion with spermatogenic impairment and male infertility in the South Chinese population. *World J Urol.* 2013;31(6):1403–1409. doi:10.1007/s00345-013-1058-7
41. Takebe M, Onohara Y, Yokota S. Expression of MAEL in nuage and non-nuage compartments of rat spermatogenic cells and colocalization with DDX4, DDX25 and MIWI. *Histochem Cell Biol.* 2013;140(2):169–181. doi:10.1007/s00418-012-1067-4
42. Wu W, Hu Y, Zhang Q, Xu Y, Su W. TNF $\alpha$  stimulates the proliferation of immature Sertoli cells by attenuating UPS-degradation of cyclin D1 and leads to the delay of BTB maturation in pubertal rats. *Andrology.* 2023;11(3):575–590. doi:10.1111/andr.13336

International Journal of Nanomedicine

Dovepress

## Publish your work in this journal

The International Journal of Nanomedicine is an international, peer-reviewed journal focusing on the application of nanotechnology in diagnostics, therapeutics, and drug delivery systems throughout the biomedical field. This journal is indexed on PubMed Central, MedLine, CAS, SciSearch<sup>®</sup>, Current Contents<sup>®</sup>/Clinical Medicine, Journal Citation Reports/Science Edition, EMBase, Scopus and the Elsevier Bibliographic databases. The manuscript management system is completely online and includes a very quick and fair peer-review system, which is all easy to use. Visit <http://www.dovepress.com/testimonials.php> to read real quotes from published authors.

Submit your manuscript here: <https://www.dovepress.com/international-journal-of-nanomedicine-journal>